Supplementary Information

White Metal-Organic Framework Nanozymes with Enzyme-Mimicking Activity Specificity: Overcoming Interferences of Color and O_2 in Colorimetric Test Strips

Lei Han, Jingying Tan, and Yucui Zhang*

College of Chemistry and Pharmaceutical Sciences, Qingdao Agricultural University, 700 Changcheng Road, Qingdao 266109, Shandong, China.

** Corresponding author.*

E-mail address: hanlei@qau.edu.cn

Contents

Experimental Section

Chemicals and Materials

$MnCl_2 \cdot 4H_2O$, OPD, TMB, ABTS, DAB and H_2O_2 were purchased from Sinopharm Chemical Reagent Co, Ltd. (China). BDC was purchased from Alfa Aesar (China). TEA, DMF and DCFH-DA were bought from Aladdin Reagent. GO_X and SO_X were purchased from Sigma Aldrich. All other reagents were of the analytical grade and used without further purification. All aqueous solutions were prepared with ultrapure water from Milli-Q system (18.2 MΩ cm).

Apparatus

The morphology of Mn-MOF nanozymes was characterized by TEM H-7650 (Hitachi, Japan) and SEM S-4800 (Hitachi,Japan). EDX spectroscopy and mapping was recorded on a spectrometer Ultim Max 40 (Oxford, UK). AFM assay was conducted by an AFM Multimode 8 (Bruker, Germany). XRD patterns were recorded on XRD D8 Advance (Bruker, Germany). XPS was performed by a spectrometer K-Alpha (Thermo Fisher Scientific, USA). The absorption spectra and the time-dependent absorbance were recorded on a microplate reader SpectraMax M2e (Molecular Devices, USA). The fluorescence was measured by fluorescence spectrophotometer F-7000 (Hitachi, Japan).

Oxidase-Like Activity Assay of Mn-MOF Nanozymes.

The analysis system of oxidase mimicking activity of Mn-MOF nanozymes was similar with the system of peroxidase-like activity, except that H_2O_2 was not added and the reaction was conducted under different atmospheres (air, O_2, and N_2) for 30 min.

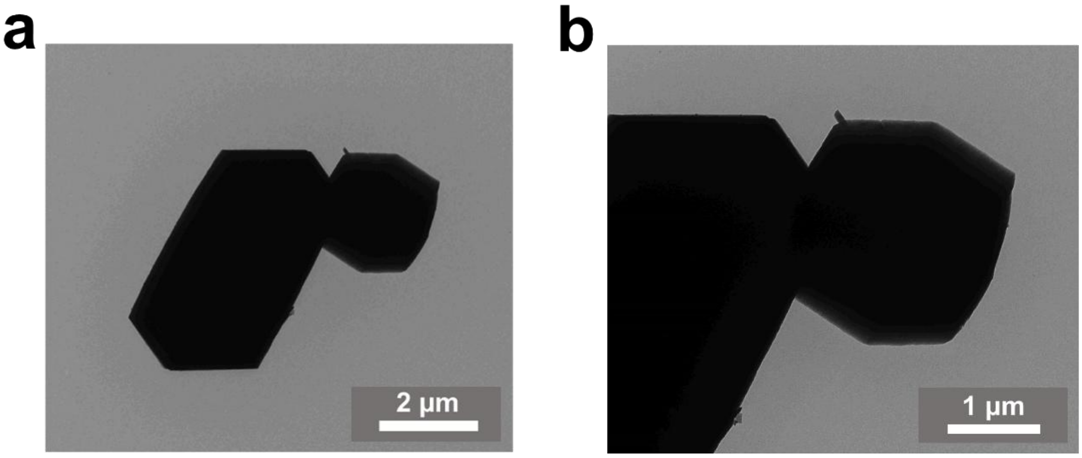

Supplementary Fig. 1. TEM image of bulk Mn-MOF.

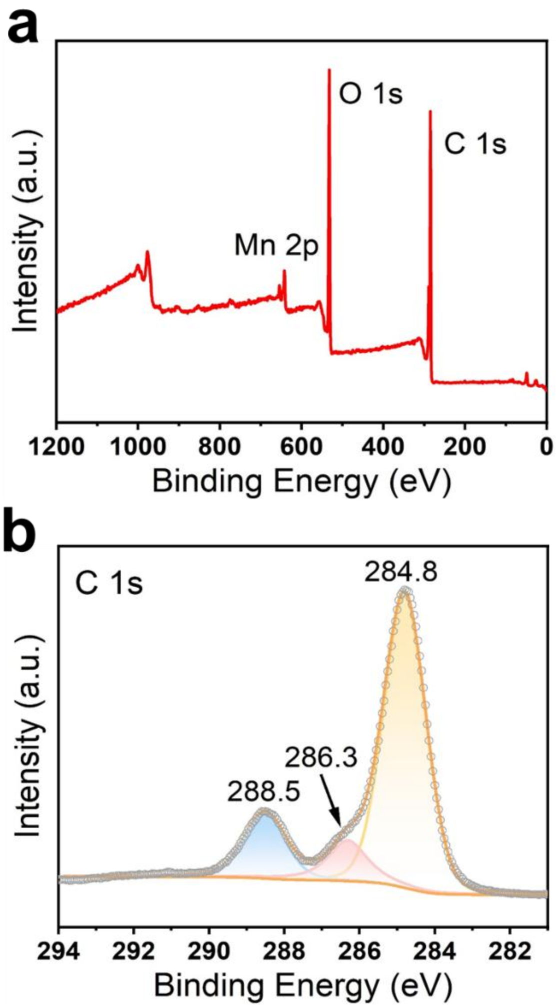

Supplementary Fig. 2. XPS spectra of Mn-MOF nanozymes. **(a)** The XPS full spectra, and **(b)** high-resolution patterns of C 1s of Mn-MOF nanozymes.

Supplementary Table 1. Colormetric parameters of different materials.

Sample [a]	CIE-$L^*a^*b^*$ parameters			WI [b]	ΔE [c]
	L^*	a^*	b^*		
Mn-TPA MOF	93.09	3.53	-0.53	93.78	0.65
Mn-ATPA MOF	69.51	10.15	7.59	46.74	23.15
Mn-TMA MOF	81.02	3.64	4.97	66.11	12.55
Co-MOF	67.38	11.52	3.45	57.03	25.36
Fe-MOF	36.45	3.39	-0.28	37.29	57.19
TiO_2	93.80	-0.70	0.20	93.20	−

a) Colorimetric parameters of TiO_2 were obtained from reference [1].

b) $WI = L^* - 3b^*$

c) $\Delta E = \sqrt{(\Delta L^*)^2 + (\Delta a^*)^2 + (\Delta b^*)^2}$

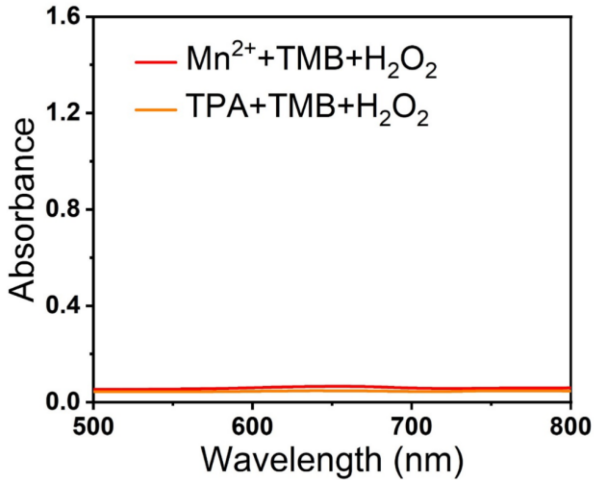

Supplementary Fig. 3. Characterization for POD-like activity of Mn^{2+} and TPA.

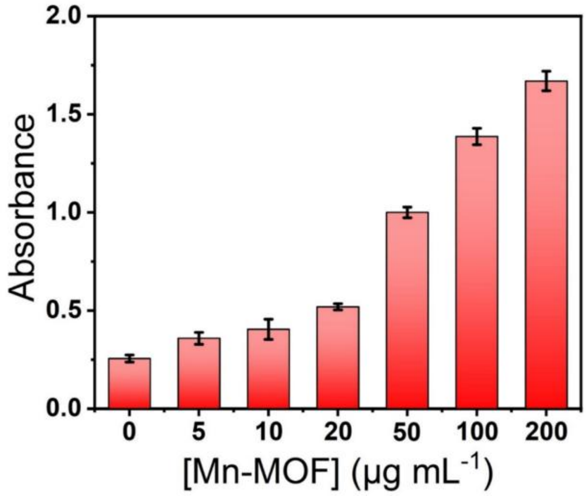

Supplementary Fig. 4. The column graphs of absorbance of TMB oxidation by different concentrations of Mn-MOF nanozymes with H_2O_2. The Absorbance of TMB with different concentrations of Mn-MOF nanozymes (0, 5, 10, 20, 50, 100 and 200 μg mL^{-1}) in the presence of H_2O_2 after incubation (0.1 M acetate buffer, pH 4.0).

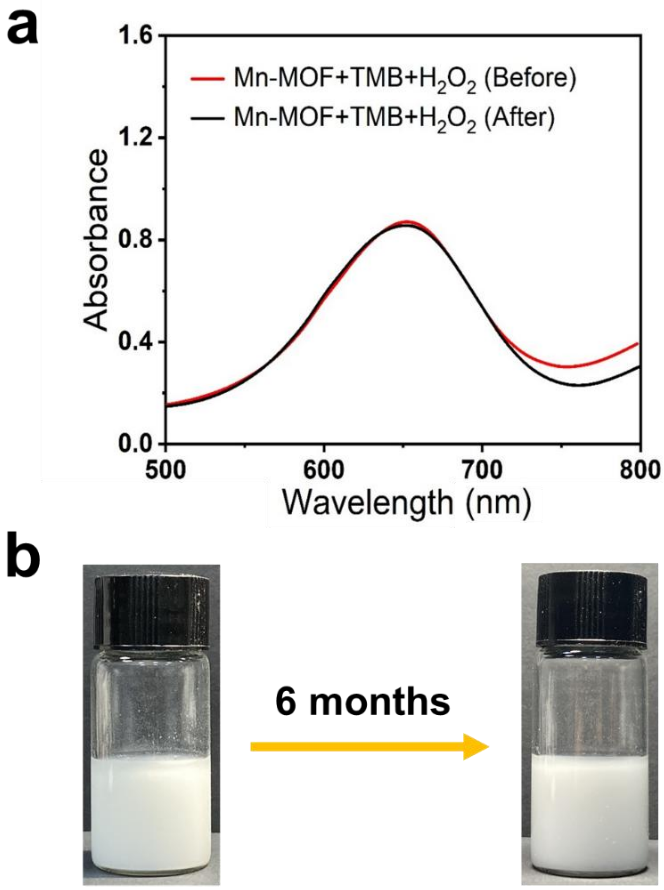

Supplementary Fig. 5. Peroxidase-like activity and photographs of Mn-MOF nanozymes before and after 6 months of storage.

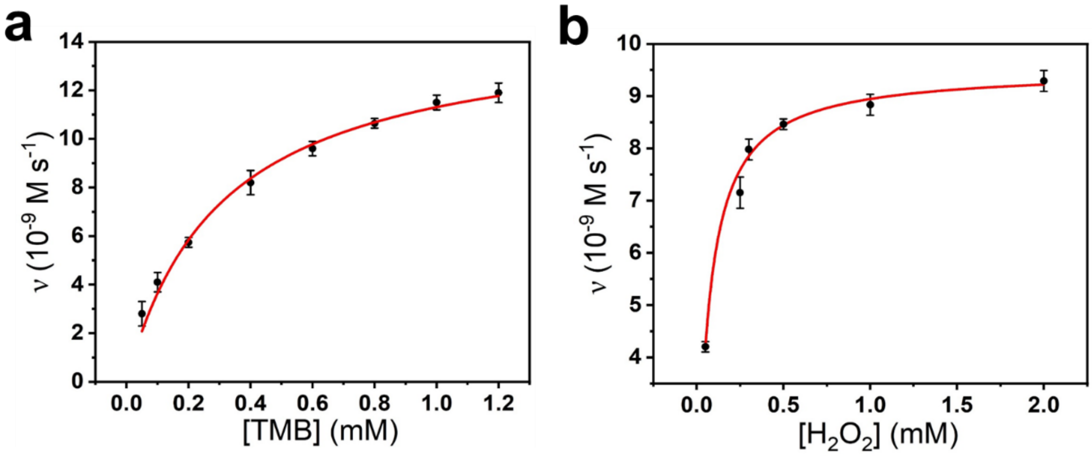

Supplementary Fig. 6. Steady-state kinetics of Mn-MOF nanozymes. Michaelis-Menten curves fit for **(a)** varied concentrations (0.05–1.2 mM) of TMB with fixed concentration (1 mM) of H_2O_2, and **(b)** varied concentrations (0.1–2 mM) of H_2O_2 with fixed concentration (0.5 mM) of TMB.

Supplementary Table 2. Comparison of K_m and V_{max} between Mn-MOF nanozymes and other catalysts.

Catalyst[a]	Substrate	K_m (mM)	V_{max} (10^{-8} M s^{-1})	Ref.
HRP	TMB	0.434	10.0	[2]
	H_2O_2	3.700	8.71	
Fe_3O_4	TMB	0.098	3.44	[2]
	H_2O_2	154	9.78	
$NiFe_2O_4$	TMB	0.550	4.57	[3]
	H_2O_2	2.600	14.11	
Co_3O_4	TMB	0.037	6.27	[4]
	H_2O_2	140.07	12.1	
CuO	TMB	25	10.49	[5]
	H_2O_2	400	16.1	
Ni-MOF nanosheet	TMB	0.365	6.53	[6]
	H_2O_2	2.490	130	
Ni-MOF	TMB	0.431	3.10	[7]
	H_2O_2	0.277	3.25	
Au/Co_3O_4-CeO_x	TMB	0.122	0.87	[8]
	H_2O_2	0.272	0.40	
GeO_2	TMB	0.420	23.40	[9]
	H_2O_2	1.750	23.40	
Mn-MOF	TMB	0.310	1.48	This work
	H_2O_2	0.063	0.95	

a) HRP, horse-radish peroxidase.

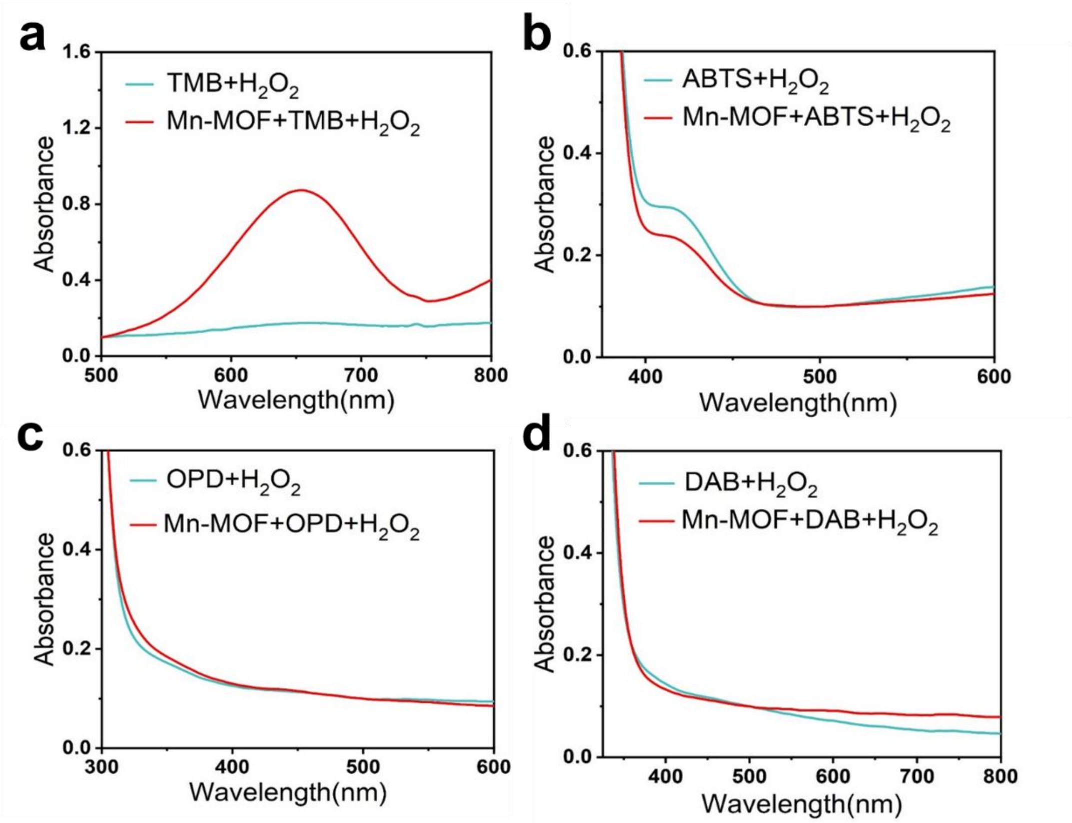

Supplementary Fig. 7. Peroxidase-like activity of Mn-MOF nanozymes for different substrates. Typical absorption spectra of **(a)** TMB, **(b)** ABTS, **(c)** OPD and **(d)** DAB oxidation catalyzed by Mn-MOF nanozymes and controls in the presence of H_2O_2 in the acetate buffer (pH 4.0, 0.1 M).

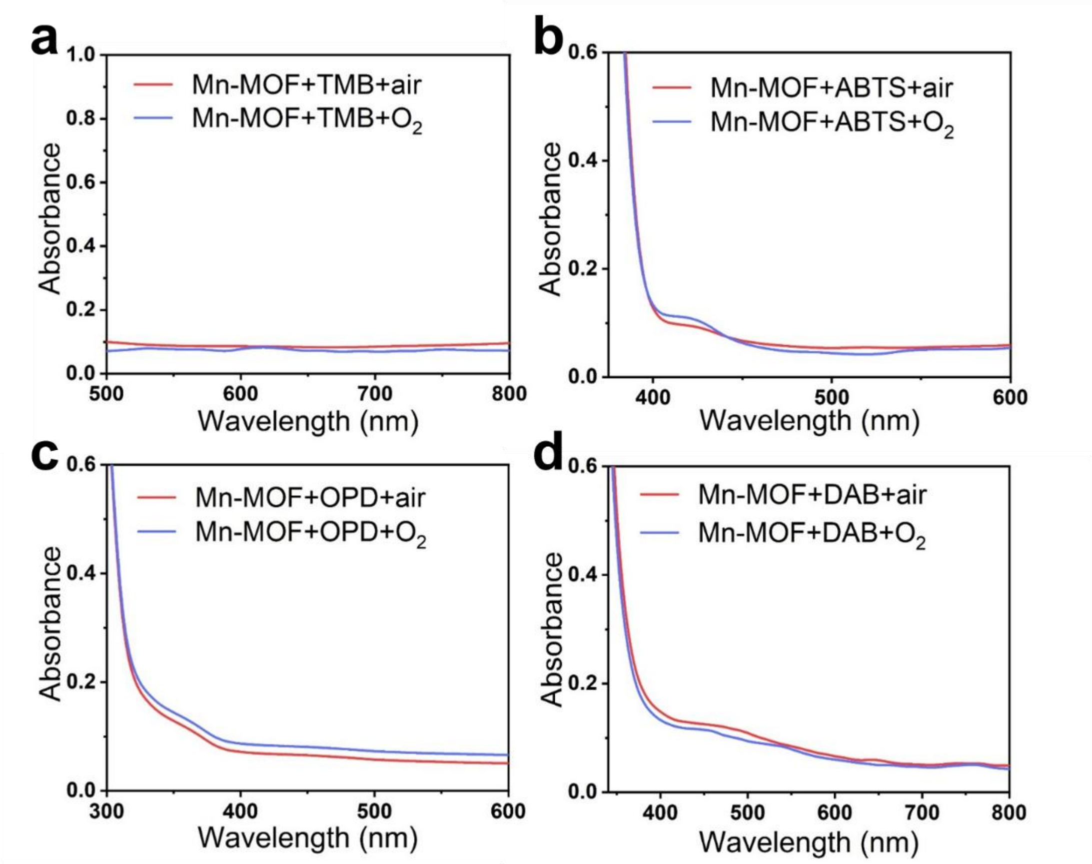

Supplementary Fig. 8. Oxidase-like activity of Mn-MOF nanozymes for different substrates. Absorption spectra of catalytic oxidation of **(a)** TMB, **(b)** ABTS, **(c)** OPD and **(d)** DAB by Mn-MOF nanozymes under air, O_2 atmosphere.

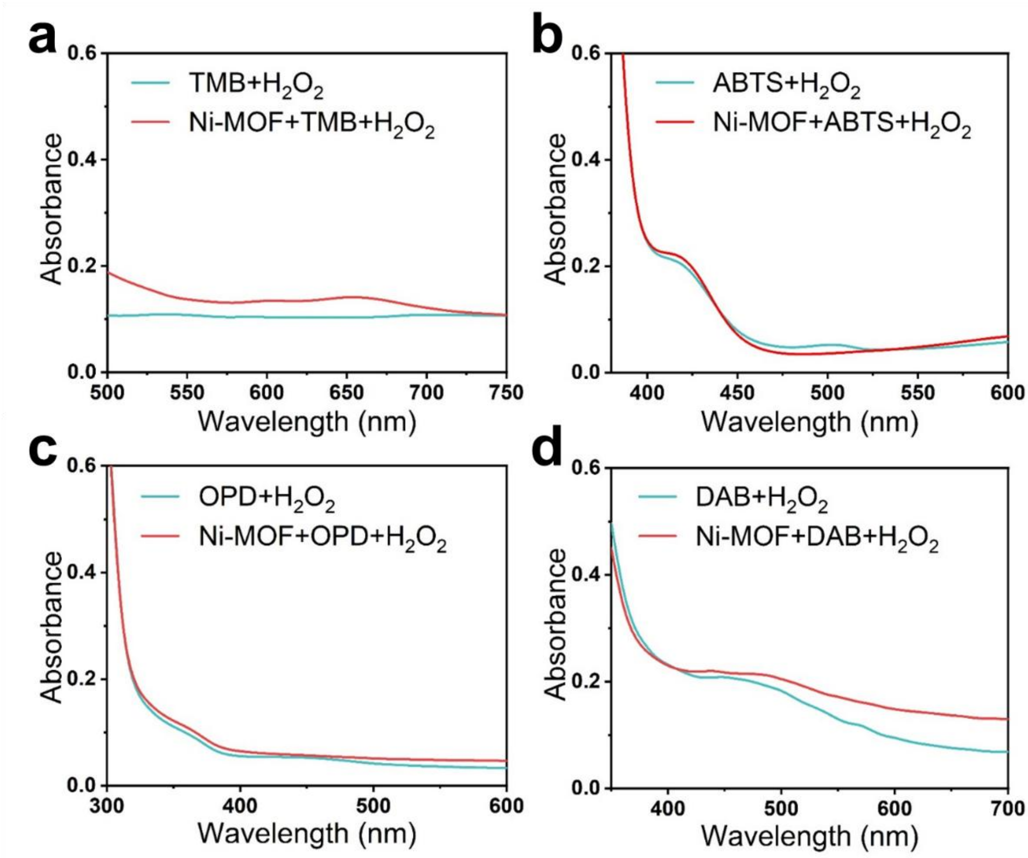

Supplementary Fig. 9. Peroxidase-like activity of Ni-MOF nanozymes. Absorption spectra of catalytic oxidation of **(a)** TMB, **(b)** ABTS, **(c)** OPD and **(d)** DAB by Ni-MOF nanozymes.

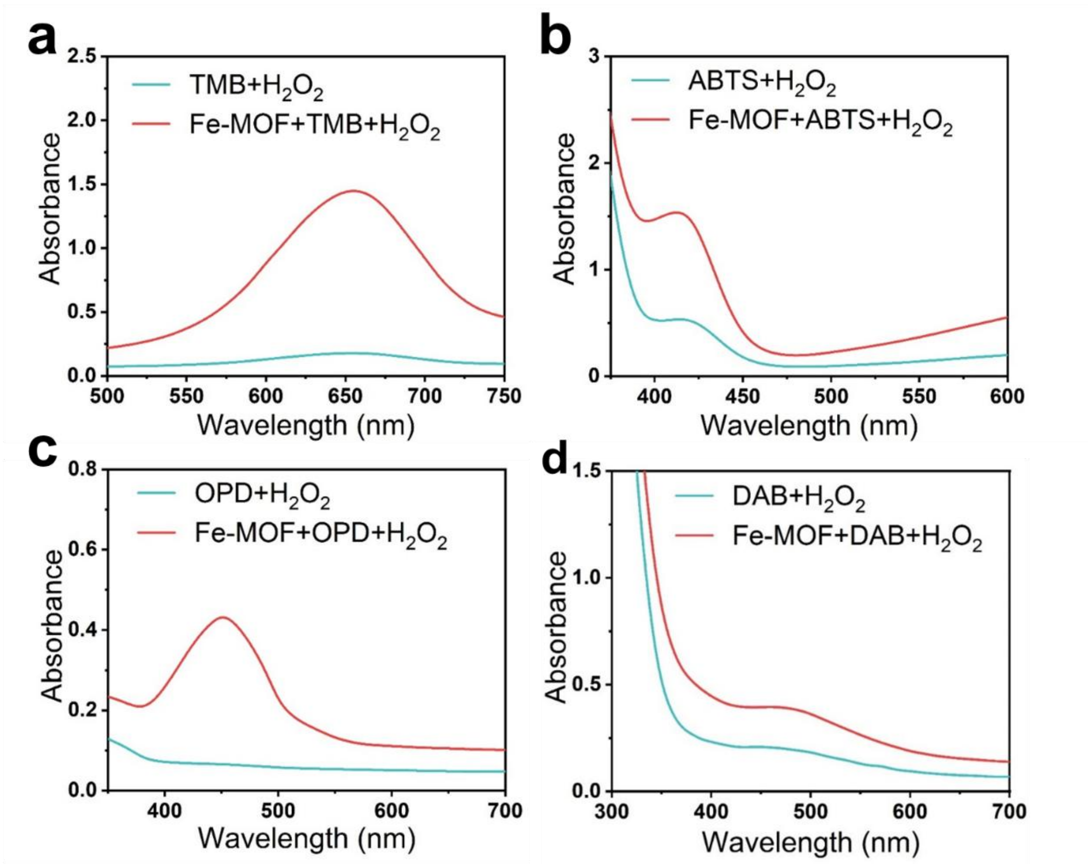

Supplementary Fig. 10. Peroxidase-like activity of Fe-MOF nanozymes. Absorption spectra of catalytic oxidation of **(a)** TMB, **(b)** ABTS, **(c)** OPD and **(d)** DAB by Fe-MOF nanozymes.

Supplementary Table. 3. Comparison of various H_2O_2 detection methods

Method[a]	Materials[b]	Linear rang	LOD	Ref.
Electrochemistry	FeMo	1–100 μM	0.81 μM	[10]
Electrochemistry	FePr	10–110 μM	4.9 μM	[11]
Electrochemistry	PBEA	5–1000 μM	1.9 μM	[12]
HSV Chromometry	MOF-818	0.033–66 mM 0.0133–10 mM	15.37μM 9.02 μM	[13]
Chromometry	Mn-MOF	5–400 μM	0.43 μM	This work

a) HSV, hue-saturation-value;

b) PBEA, prussian blue-based electrode array.

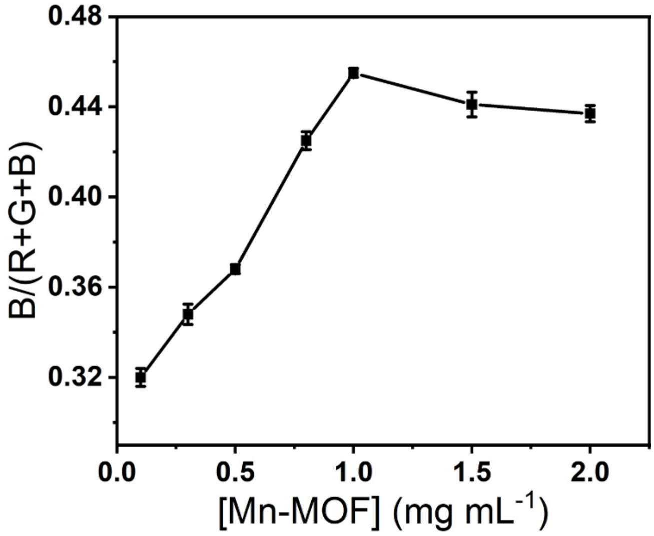

Supplementary Fig. 11. The concentration optimization of Mn-MOF nanozymes on test strip.

Supplementary Table 4. Comparison of various glucose detection methods.

Method	Materials[a]	Linear rang	LOD	Ref.
Electrochemistry	PGO_x@MXene/CS	0.03–16.5 mM	3.1 μM	[14]
Electrochemistry	CoOOH@Cu	0.025–2.5 mM	7.38 μM	[15]
Chromometry		0.025–2.5 mM	2.07 μM	
Chromometry	$TiSe_{2-x}$@Au	0.015–0.6 mM	3.7 μM	[16]
Chromometry	PGA-Fe/CS	20–600 μM	2.4 μM	[17]
Chromometry	Fe SSN	10–60 μM	2.1 μM	[18]
Chromometry	Mn-MOF	5–600 μM	0.49 μM	This work

[a)] PGOx, GOx polynanogel; CS, chitosan; PGA, poly-γ-glutamic acid; Fe SSN, single iron site nanozymes.

Supplementary Table 5. Comparison of various sarcosine detection methods.

Method	Materials[a]	Linear rang	LOD	Ref.
Electrochemistry	$CuInS_2$	10–1000 μM	8.0 μM	[19]
Fluorescence	CuT@N/Au	10–1100 μM	4.7 μM	[20]
Chromometry	Fe_3O_4@SiO_2@$NiCo_2S_4$	1.25–350 μM	0.42 μM	[21]
Chromometry	NQS/GO	6.2–263 μM	0.73 μM	[22]
Chromometry	Fe-doped g-C_3N_4	10–500 μM	3.6 μM	[23]
Chromometry	Mn-MOF	5–300 μM	0.27 μM	This work

a) CuT, tryptophan-based Cu-containing; NQS, 1,2-naphthoquinone-4-sulphonic acid sodium salt; GO, graphene oxide.

Supplementary References

[1] Wang, Y., Mumford, K. A., Shen, S. & Li, Y. *Powder Technology* **2015**, 284, 204-209.

[2] L. Gao, J. Zhuang, L. Nie, J. Zhang, Y. Zhang, N. Gu, T. Wang, J. Feng, D. Yang, S. Perrett, X. Yan, *Nature Nanotechnology* **2007**, 2, 577.

[3] L. Su, W. Qin, H. Zhang, Z. U. Rahman, C. Ren, S. Ma, X. Chen, *Biosensors and Bioelectronics* **2015**, 63, 384.

[4] J. Mu, Y. Wang, M. Zhao, L. Zhang, *Chemical Communications* **2012**, 48, 2540.

[5] J A. P. Nagvenkar, A. Gedanken, *ACS Applied Materials & Interfaces* **2016**, 8, 22301.

[6] Chen, Y. Shu, H. Li, Q. Xu, X. Hu, *Talanta* **2018**, 189, 254.

[7] J. Guo, Y. Liu, Z. Mu, S. Wu, J. Wang, Y. Yang, M. Zhao, Y. Wang, *Microchimica Acta* **2022**, 189, 219.

[8] H. Liu, Y. Ding, B. Yang, Z. Liu, Q. Liu, X. Zhang, *Sensors and Actuators B: Chemical* **2018**, 271, 336.

[9] X. Liang, L. Han, *Advanced Functional Materials* **2020**, 30, 2001933.

[10] H. Li, Q. Cai, J. Wang, G. Jie, *Biosensors and Bioelectronics* **2023**, 232, 115315.

[11] K. Niu, J. Chen, X. Lu, *Chemical Engineering Journal* **2023**, 475, 146491.

[12] D. Rojas, J. F. Hernández-Rodríguez, F. Della Pelle, M. Del Carlo, D. Compagnone, A. Escarpa, *Biosensors and Bioelectronics* **2020**, 170, 112669.

[13] K. Yu, M. Li, H. Chai, Q. Liu, X. Hai, M. Tian, L. Qu, T. Xu, G. Zhang, X. Zhang, *Chemical Engineering Journal* **2023**, 451, 138321.

[14] X. Tong, L. Jiang, Q. Ao, X. Lv, Y. Song, J. Tang, *Biosensors and Bioelectronics* **2024**, 248, 115942.

[15] H. Cheng, Z. Wang, H. Sun, B. Chen, J. Huang, R. Jia, X. He, K. Wang, *Chemical Communications* **2022**, 58, 13487.

[16] C. Sun, X. Zhang, H. Huang, Y. Liu, X. Mo, Y. Feng, J. Wang, W. Zhou, P. K. Chu, X.-F. Yu, W. Liu, *Biosensors and Bioelectronics* **2023**, 241, 115665.

[17] Q. H. Nguyen, D. H. Lee, P. T. Nguyen, P. G. Le, M. I. Kim, *Chemical Engineering Journal* **2023**, 454, 140541.

[18] M. Chen, H. Zhou, X. Liu, T. Yuan, W. Wang, C. Zhao, Y. Zhao, F. Zhou, X. Wang, Z. Xue, T. Yao, C. Xiong, Y. Wu, *Small* **2020**, 16, 2002343.

[19] X.-Y. Jiang, L. Zhang, Y.-L. Liu, X.-D. Yu, Y.-Y. Liang, P. Qu, W.-W. Zhao, J.-J. Xu, H.-Y. Chen, *Biosensors and Bioelectronics* **2018**, 107, 230.

[20] M. Wang, L. Zhang, X. Zhou, J. Zhang, C. Zhou, X. Su, *Analytica Chimica Acta* **2022**, 1223, 340188.

[21] X. Wang, M. Chen, L. Zhao, *Chemical Engineering Journal* **2023**, 468, 143612.

[22] Z. Xue, B. Yin, H. Wang, M. Li, H. Rao, X. Liu, X. Zhou, X. Lu, *Nanoscale* **2016**, 8, 5488.

[23] X. Xi, X. Peng, C. Xiong, D. Shi, J. Zhu, W. Wen, X. Zhang, S. Wang, *Microchimica Acta* **2020**, 187, 383.